HUNTINGTON MEDICAL RESEARCH INSTITUTES
NEURAL ENGINEERING LABORATORY
734 Fairmount Avenue
Pasadena, California 91105

Contract No. N01-NS-1-2340
Quarterly Progress Report
Oct 1-Dec 31, 2001
Report No. 1

"Functional Microstimulation of the Lumbosacral Spinal Cord"

Douglas McCreery, Ph. D.
Albert Lossinsky, Ph.D.
Victor Pikov, Ph.D
William Agnew, Ph.D
Leo Bullara, B.A.

ABSTRACT

The objective of this project is to develop neuroprostheses that will allow patients with severe spinal cord injuries to regain control of their bladder and bowel. The approach is based on an array of microelectrodes that is implanted into the sacral spinal cord.

Three arrays of 9 activated iridium microelectrodes were implanted into the S_2 levels of the sacral spinal cord of 3 cats (SP128,SP129, SP130) using the high-speed inserter tool. For chronic stimulation, the cats were lightly anesthetized with Propofol and we used stimulus parameters which had induced relaxation of the EUS during the urodynamic measurements. Three electrodes were pulsed for a total of 24 hours (12 hrs/day) on two successive days. The stimulus waveform was cathodic-first, controlled-current, charge-balanced (biphasic) pulse pairs, 100 :A in amplitude and 400 :s in duration, at 20 Hz. We used a 10% duty cycle (repeated cycles of 60 seconds of stimulation, then 540 seconds without stimulation). At the end of the 2nd day, the cats were deeply anesthetized and perfused with fixative for histologic evaluation of the electrode sites. The tissue sections were stained for the specific neuronal nuclear protein NeuN.

In cats SP128 and SP129, we examined 8 pulsed electrode sites, and 10 that were not pulsed, except to perform the urodynamic measurements. The pulsed electrode had received 12 hours of pulsing per day on each of 2 successive days. The charge per phase was 40 nC, the charge density was 2,000 :C/cm². The pulse frequency was 20 Hz with a 10% duty cycle (1 minute of stimulation; 9 minutes without stimulation repeated indefinitely). The distribution of neurons around the pulsed and unpulsed neuron electrodes appeared similar by inspection, with a tendency for the number of neurons to decrease within 100 :m of the pulsed tips. We did note accumulations of inflammatory cells near the tips of 2 of the pulsed electrodes, accompanied by perivascular cuffing of nearby vessels. However, in all cases, there were viable neurons within 100 :m of all of the pulsed and unpulsed electrodes.

Overall, the NeuN immunohistochemical stain with Nissl counter-stain is proving to be very helpful as we characterize the tissue responses to chronically-implanted intraspinal microelectrodes and develop penetrating microelectrodes which inflict less injury. The Nissl- NeuN combination clearly delimits the extent of the gliotic scars that often occur ventral to the electrode tips and clearly reveals the distribution of neurons near the margin of the scars as well as in the surrounding neuropil. The brown-stained neurons are clearly differentiated from the astrocytes, microglia and any infiltrated inflammatory cells.

We also noted evidence of spalled iridium or iridium oxide at the sites of 3 of the 8 pulsed electrode tips. This does suggest that the threshold for exfoliation of iridium from anodically-biased activated iridium microelectrodes is closer to 2,000 :C/cm² than to 3,000 :C/cm². The evidence from previous animals supports this conclusion. We should note that we have been using blunt-tip microelectrodes (tip radii of curvature = 5 - 6 :m) which would be expected to encourage a quite uniform current distribution over the electrode's exposed surface. In the next animal, we will be evaluating electrodes with radii of curvature or 3 - 4 :m, to determine if the sharper tips will affect the gliotic scarring and neovascularization beneath the chronically-implanted electrodes. However, the sharper tips will encourage nonuniform current distributions if the exposed sites are at the electrode tips, and the non-uniform current density may make these electrodes even more susceptible to erosion and exfoliation of iridium. The solution may be to place the active electrode sites on the sides of the shafts rather than at their tips.

Overall, the amount of tissue injury seen in these two animals appears to be sufficiently minor so as not to compromise the functionality of the spinal cord. The NeuN stain revealed neurons within a few microns of most of the unpulsed tips, and within 100 :m of the pulsed tips. Indeed, in cat SP130, which is yet to be sacrificed, we were able to record action potentials from single neural units, from 8 of the 9 microelectrodes, at 35 days after implantation of the array. The amount of mechanical injury induced by these larger (75 :m diameter) electrodes certainly is no greater than that inflicted by the 50- :m shafts that we used earlier, and the heavier shafts are more resistant to damage during handling in the operating room, when the array must be removed from its protective enclosure and loaded into the inserter tool.

In both SP128 and SP129, the electrode tips were located either dorsal to the central gray commissure, or in the intermediate horn. None of the electrodes was able to induce a sustained increase in bladder pressure, although many were able to induce relaxation of the urethral sphincter. At least one of the electrodes (electrode 6 in cat SP128) also was able to suppress spontaneous contractions of the bladder, and this is one of the objectives of our contract. In subsequent arrays, the span of the array will again be 1.8 mm, an in our original design.

METHODS

The objective of this project is to develop neuroprostheses that will allow patients with severe spinal cord injuries to regain control of their bladder and bowel. The system is based on an array of microelectrodes that is implanted into the sacral spinal cord. The procedures and hardware are being developed in cats with intact spinal cords, and in the 2nd year of the project, the implanted cats will undergo transection of the spinal cord at the low thoracic level.

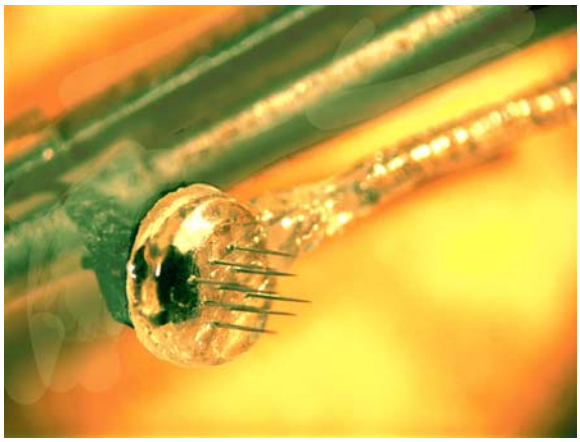

Figure 1

Fabrication and implantation of the arrays

Previously we have used arrays of 6 activated iridium microelectrodes extending from an epoxy superstructure whose underside is curved to conform to the curvature of the feline sacral spinal cord. In the present series, we added 3 electrodes along the midline of the array, in order to provide better access to the neurons of the central gray commissure, which inhibit the motoneurons innervating the external urethral sphincter (EUS). The left-to right spacing between the outboard electrodes also was reduced to 1.0 mm (from 1.6 mm in our previous arrays), so that the outboard electrodes would reside closer to the midline of the cord. It was our expectation that they could then activate axons from the CGS that inhibit the EUS, or activate the neurons of the sacral parasympathetic nucleus that mediate contraction of the bladder vesicle. Also, the diameter of the microelectrodes was slightly greater (75 ：m) than in previous arrays (50 ：m), in order to reduce the risk of damaging them during the implant procedure. An array of this type is shown in Figure 1. It was recovered from the spinal cord of cat SP129, 34 days after implantation.

One array each was implanted into the sacral spinal cords of cat SP128 ,SP129 and SP130. The sacral cord was exposed using a standard dorsal laminectomy. We stimulated the perigenital skin, and recorded at each of several locations along the dorsal surface of the sacral cord. In SP129 and SP130, the array was implanted near the maximum of the 2nd component of the evoked response (the dorsal cord potential). In SP128, it was implanted about 4 mm caudal of the maximum. At autopsy, the position of the array was validated by complete dissection of the spinal roots and was found to be at the caudal S_2 level in cat SP128 and at the caudal S_2 level in cat SP129. Cat SP130 is still living.

The arrays were inserted with the high-speed inserter tool at a velocity of approximately 1 m/sec. The dura was then closed over the array, using 5 pre-installed sutures.
Cats SP128 and SP129 were deeply anesthetized with pentobarbital, given i.v. heparin and perfused through the aorta for 3 minutes with a prewash solution consisting of 900 ml of phosphate-buffered saline, and 0.05% procaine HCl. The animal were flushed with 4 L of a fixative containing 4% formalin and 0.25% glutaraldehyde in 0.1 M sodium phosphate buffer. The cats were refrigerated overnight until autopsies were performed on the following day. Fixation of the spinal cord was good and the electrode arrays were determined neuroanatomically to be positioned within S_2.

Tissue blocks containing both the microelectrodes and areas rostral and caudal to the electrodes were washed overnight in 4% formalin, then in distilled water for 2 hrs, dehydrated in a graded series of ethanol and embedded in paraffin. The paraffin-embedded tissue blocks were cut at a thickness of 6-7 μm and 4 sections were picked up on each histogrip-coated-slide. These slides were routed either for routine histologic staining with Nissl, or for immunohistochemistry.

NeuN Immunohistochemistry. We performed immunohistochemistry for NeuN, on tissue sections containing either the electrode tips, or sections 8-32 μm caudal or rostral to the electrode tips. This antibody recognizes many vertebrate neuron-specific proteins within the nuclei (primarily) and neuronal cytosol (to a slightly lesser degree) within the CNS of humans, rats, mice, chickens, ferrets and salamanders. The mouse has been extensively studied and positive staining occurs in neuronal populations in the cerebellum, cerebral cortex, hippocampus, thalamus, spinal cord and neurons in the peripheral nervous system including dorsal root ganglia, sympathetic chain ganglia and enteric ganglia. Unreactive cell types include Purkinje, mitral and photoreceptor cells. The results of our experiments on SP128 and SP 129 demonstrate positive labeling of neurons near and adjacent to pulsed and unpulsed electrodes of the spinal cord.

NeuN Labeling. Sections were deparaffinized, rehydraded in a decreasing ethanol series and washed in PBS. We employed an antigen retrieval technique in which the sections on glass slides were microwaved for 12 minutes at 70% in acidic citrate buffer, 3 sessions at 4 min each, adding acid citrate buffer as needed. After cooling, tissue sections were rinsed 3 X in distilled H_2O, then changed to PBS buffer for a 5 min rinse, quenched with 0.1M NH_4Cl for 10 min to remove unbound aldehyde groups, rinsed in PBS 5 min and treated with 1% H_2O_2- Methanol-PBS mixture for 30 minutes to remove endogenous peroxidase activity. All incubations were carried out in a humidifying chamber (plastic sandwich container containing wet paper towels and lid) at 25°C. The sections were then rinsed 5 min in PBS and then blocked with PBS containing 50% goat serum for 1 hr at 25°C. After blotting, the sections were reacted with anti-NeuN antibody diluted 1:50 in PBSS (PBS containing 10% goat serum). After thorough washing with PBS (wash bottle rinse for 30 seconds), the tissue sections were incubated with a secondary antibody consisting of 1:50 dilution (in PBSS) of biotinylated goat anti-mouse IgG H+L 1 hr at 25°C, then washed with PBS 30 seconds. The sections were than incubated with a 1:50 dilution of exrtravidin HRP for 1 hr at 25° C, then rinse again with PBS for 30 sec. The reverse sides of the slides are wiped off and cytochemically reacted with 0.05 M 3, 3'-diaminobenzidine tetrahyrochloride containing 0.05% H_2O_2 in 0.05 M TRIS buffer, pH: 7.6 for 1-5 min at 25°C. After final rinsing in PBS, the tissue sections were lightly counter stained with Nissl. We used cerebral cortex and cochlear nucleus tissue sections as positive control material because of their excellent NeuN staining.

RESULTS

Measurements of bladder and sphincter pressure

At 54 days (Cat SP128) or at 34 days (SP129) after implanting the array, we determined the effect of microstimulation in the sacral cord on the hydrostatic pressure within the urinary bladder and on the tone of the urethral sphincter. The cat was anesthetized with Propofol and the urinary bladder was catheterized. Hydrostatic pressure within the bladder vesicle was measured with a micro-transducer (Miller Instruments, Model SPR524), using the apparatus depicted in Figure 2, and the data were digitized and stored in a PC computer. The bladder was evacuated, then filled with sterile saline by elevating the open-top reservoir to a height of 20 cm above the bladder. The constrictive force within the external urethral sphincter (EUS) was measured as an "infusion pressure"; the resistance to the infusion of saline through a port on the side of the catheter as saline was infused continuously at a rate of 100 ml/hr.

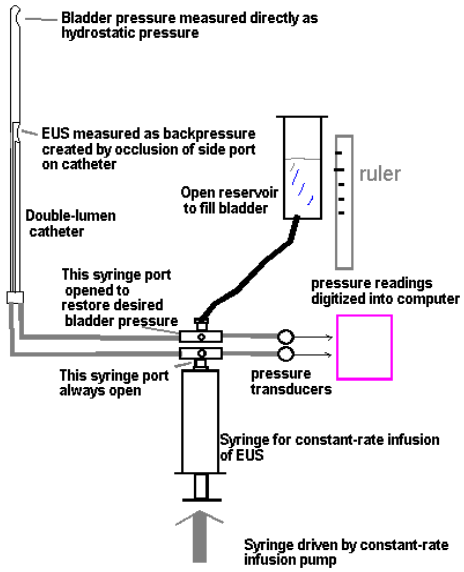

Figure 2

In cats SP128 and SP129, electrical stimulation via 1 or more of the electrodes induced marked relaxation

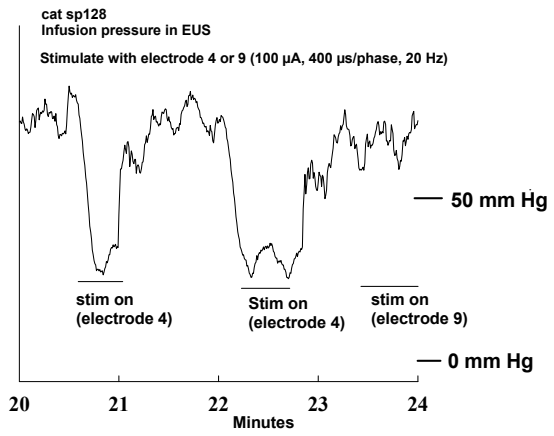

Figure 3

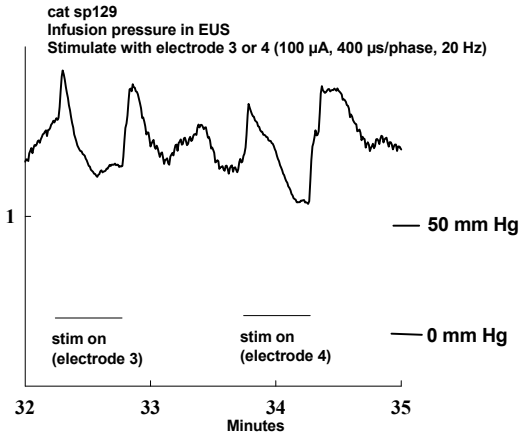

Figure 4

of the EUS (Figures 3 and 4). In SP128, electrodes 1, 4 and 6 produced sufficient relaxation of the EUS to allow the cat to urinate. In SP129, electrodes 3, 4 and 5 produced marked relaxation of the sphincter. Figure 3 from cat SP128 illustrates the spatial specificity of the electrical stimulation, a phenomenon that we have reported previously. Electrode 4 (which was near the

midline of the cord, and above the central canal, induced a marked relaxation of the EUS while electrode 5, which was only 1,000 μm rostral, and slightly lateral of electrode 1, produced no effect. This spatial specificity is quite remarkable in view of the high stimulus charge per phase.

In cat SP129, interleaved (sequential) pulsing of electrodes 3 and 4 produced a small increase in bladder pressure, which was not sustained though the interval of stimulation (Figure 5). In cat SP128, none of the electrodes produced more than a very small increase in pressure within the bladder vesicle. However, stimulating with electrode 6 (which was close to the central canal of the cord) did inhibit spontaneous contractions of the bladder (Figure 6). The inability of the stimulus to induce effective contraction of the bladder detrusor implies that the electrodes were too close to the midline of cord, and this is confirmed by the histologic findings presented below. In these arrays, the left-to-right span of the array was 1.0 mm. We have modified the

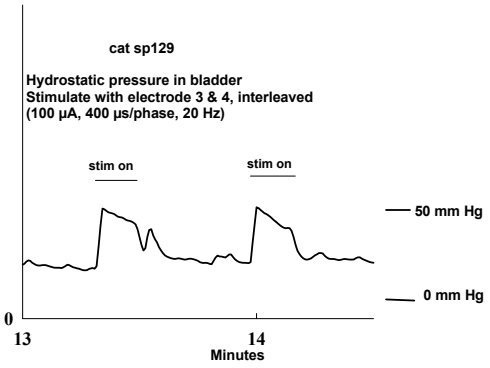

Figure 5

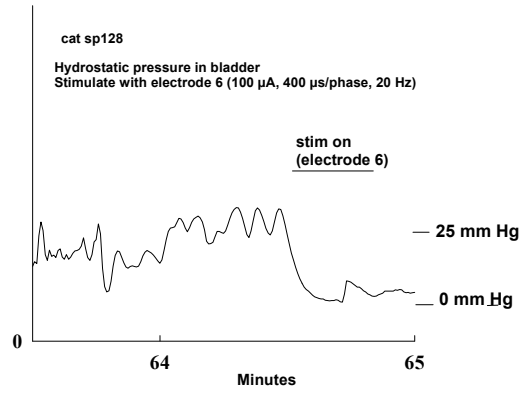

Figure 6

array mold so that in subsequent animals, the outboard electrodes will span 1.7 mm, as in our original design

Chronic stimulation protocol

The stimulation regimen was conducted on the 34th and 35th day after implantation of the array into cat SP128. For cat SP129, the stimulation was conduced on the 51th and 52nd day. The cats were lightly anesthetized with Propofol. Electrodes 1, 3 and 4 in cat SP128 and electrodes 1,3,4,5 and 7 in cat SP129 were pulsed for a total of 24 hours (12 hours on each of two successive days), all with the same stimulus parameters. The stimulus waveform was cathodic-first, controlled-current, charge-balanced (biphasic) pulse pairs, 100 μA in amplitude and 400 μs in duration, at 20 Hz per electrode. In a clinical prosthesis, continuous stimulation would not be required for periodic evacuation of the urinary bladder. Thus we used a 10% duty cycle (repeated cycles of 1 minute of stimulation, then 9 minutes without stimulation). This stimulus was administered for 12 hours on each of two successive days.

At the end of the 2nd day of stimulation, the cats were deeply anesthetized with pentobarbital, given i.v. heparin and perfused through the aorta for 3 minutes with a prewash

solution consisting of 900 ml of phosphate-buffered saline, and 0.05% procaine HCl. This was followed by a fixative containing 4% formalin and 0.25% glutaraldehyde in 0.1 M sodium phosphate buffer. The sacral spinal cord was resected and the capsule of connective tissue covering the epoxy array superstructure was removed, leaving the array *in situ.* The spinal roots and nerves were identified to determine the exact level of the array.

Histologic and Immunohistochemistry

Nine electrode tips from each cat (SP128 and SP129) were located in the S_1 - S_2 spinal cord. The array in SP128 was inserted on the left side of the cord, and the shafts were angled slightly to the left. In SP129, the array was well centered over the midline of the sacral cord and the electrodes were oriented vertically. Neither animal presented evidence of hemorrhage near the electrode tracks but there were gliotic scars beneath some of the electrodes in both cats. In both animals, there were minor inflammatory reactions including vasculitis and perivascular cuffs, and infiltration of inflammatory cells near some of the pulsed electrodes. The inflammatory cells consisted primarily of small, round lymphocytes. Neovascularization was a common feature in association with all electrode tracks.

SP 128. This array was inserted into the left side of the cord at the S_2 level. Three of the electrode tips (electrodes 4,5,6) were located within the dorsal horns. Two electrodes were within the lateral white column (electrodes 1 and 3) and one was within the junction between the dorsal horn and the lateral white column (electrode 2). The remaining three middle electrodes (electrodes 7,8,9) were located within or near the central gray commissure. Unpulsed electrodes (electrodes 2, 5,6,7,8,9) were surrounded by NeuN-positive neurons, within a few microns of the electrode tips and shaft (Figures 7,11,12). The shafts and tips of pulsed electrodes (electrodes1,3,4) also were surrounded by NeuN-positive neurons and their processes (Figures 8,9,10). The NeuN-stained neurons were much more conspicuous than in the adjacent sections that were stained with Nissl alone (compare Figures 9 and 10). A few leukocytes surrounded the capsules of the pulsed electrodes, as seen in the sections stained with Nissl alone (Figure 9), and also in sections stained with NeuN and counter stained with Nissl (Figure 10). The capsules surrounding unpulsed electrodes were composed primarily of glial cells and few leukocytes (Figure 11, 12.)

SP129. The array was well-centered above the midline of the cord, and tips of the six outboard electrodes (electrodes 1-6) were positioned within the intermediate horns. The tips of the three central electrodes (electrodes 7,8,9) were within, or slightly dorsal to, the central gray commissure and dorsal to the central canal (Figure 13). Similar to the immunohistochemical staining observed in SP128, NeuN-positive neurons and their processes were distributed around both pulsed and unpulsed electrodes. Neovascularization was also observed around and ventral to several the electrode shafts (Figures 14,15,17). In this animal there was more infiltration of leukocytes than in SP128, within the tissues surrounding some of the pulsed electrodes (Figure 19) but not the unpulsed electrodes. Some blood vessels adjacent to the pulsed electrodes exhibited vasculitis (Figures 14,16,18) and a few perivascular cuffs were observed in association with pulsed, but not unpulsed electrodes (Figure 19). Although this array was not tilted, gliotic

scars extended ventral of 3 of the electrodes (Figures 15, 17, 19).

DISCUSSION

NeuN immunoreactivity produced staining of neuronal nuclei cytosol , and neuronal processes within the gray matter surrounding the electrodes. The neuropil of the spinal gray matter was weakly NeuN-positive. This may be non-specific staining, or it may reflect staining of numerous minute neuronal processes (Figures 10, 12, 19). The brown color of the HRP-DAB chromagen immunochemically linked to the NeuN protein epitopes enabled us to clearly differentiate neurons from all other cell types including glia, endothelium and leukocytes, which all stained a blue color with the Nissl stain (Figures 10,11,12,14,15,16,17,18). In some cases, however, the edendymal cells surrounding the central canal stained a light brown color. This possible non-specific staining was variable and is not clearly understood. We are evaluating the non-specific immunoreactivity of the ependymal cells with anti-NeuN antibody. In the next quarter, we plan to conduct titration experiments on control spinal cord tissues from SP128 and SP129, as well as other animals using various concentrations of goat serum blocker, with and without the addition of bovine serum albumin.

Overall, the NeuN immunohistochemical stain with Nissl counter-stain is proving to be very helpful as we characterize the tissue responses to chronically-implanted intraspinal microelectrodes and develop penetrating microelectrodes which inflict less injury. The Nissl-NeuN combination clearly delimits the extent of the gliotic scars that often extend ventral to the electrode tips and the combined stains reveal the distribution of neurons near the margin of the scars as well as in the surrounding neuropil. The brown-stained neurons are well differentiated from the astrocytes, microglia and any infiltrated inflammatory cells.

In cats SP128 and SP129, we examined 8 pulsed electrode sites, and 10 that were not pulsed, except to perform the urodynamic measurements. The pulsed electrode had received 12 hours of pulsing per day on each of 2 successive days. The charge per phase was 40 nC, and the charge density was 2,000 ：C/cm². The pulse frequency was 20 Hz with a 10% duty cycle (1 minute of stimulation; 9 minutes without stimulation repeated indefinitely). The distribution of neurons around the pulsed and unpulsed neuron electrodes appeared similar by inspection, with a tendency for there to be fewer neurons within 100 ：m of the pulsed tips. We have not yet attempted to quantify this difference, primarily because the normal distribution of neuronal types and their densities within the spinal cord is very variable from one part of the cord to the other and between Rexed laminae. We did note accumulations of inflammatory cells near the tips of 2 of the pulsed electrodes, accompanied by perivascular cuffing of nearby vessels. However, in all cases, there were viable neurons within 100 ：m of all of the pulsed and unpulsed electrodes.

It is also quite clear that the NeuN stain does not differentiate between healthy and damaged neurons, but only between neurons and other cell types. Thus, we noted at least 2 NeuN-stained neurons with the eccentric nuclei that is characteristic of early chromatolysis. In the next cat, we will allocate some slides for staining with Fluor-jade B which specifically stains degenerating neurons.

We also noted evidence of spalled iridium or iridium oxide at the sites of 3 of the 8

pulsed electrode tips (Figures 14 and 16). This does suggest that the threshold for exfoliation of iridium from anodically-biased activated iridium microelectrodes is closer to 2,000 :C/cm² than to 3,000 :C/cm². The evidence from previous animals supports this conclusion. We should note that we have been using blunt-tip microelectrodes (tip radii of curvature = 5-6 :m) which would be expected to encourage a uniform current distribution over the electrode's exposed surface. In the next animal, we will be evaluating electrodes with tip radii of curvature of 3-4 :m to determine if the sharper tips will reduce (or exacerbate) the gliotic scarring and neovascularization beneath the chronically-implanted electrodes. However, the sharper tips will encourage nonuniform current distributions if the exposed sites are at the electrode tips, and the non-uniform current density may make these electrodes even more susceptible to erosion and exfoliation of iridium. The solution may be to place the active electrode sites on the sides of the shafts rather than at their tips.

Overall, the amount of tissue injury in these two animals appears to be sufficiently minimal so as not to compromise the functionality of the spinal cord. The NeuN stain revealed neurons within a few microns of most of the unpulsed tips, and within 100 :m of the pulsed tips. Indeed, in cat SP130, which is yet to be sacrificed, we were able to record action potentials from single neural units from 8 of the 9 microelectrodes, at 35 days after implantation of the array. The amount of mechanical injury induced by these larger (75 :m diameter) electrodes certainly is no greater than that inflicted by the 50-:m shafts that we used earlier, and the heavier shafts are more resistant to damage during handling in the operating room, when the array must be removed from its protective enclosure and loaded into the inserter tool.

In both SP128 and SP129, the electrode tips were located either dorsal to the central gray commissure, or in the intermediate horn. None of these was able to induce a sustained increase in bladder pressure, although many were able to induce relaxation of the urethral sphincter. At least one of the electrodes (electrode 6 in cat SP128) also was able to induce relation of spontaneous contractions of the bladder, and this is one of the objectives of our contract. In subsequent arrays, the spacing between the outboard rows of electrodes will be 1.7 mm, an in our original design.

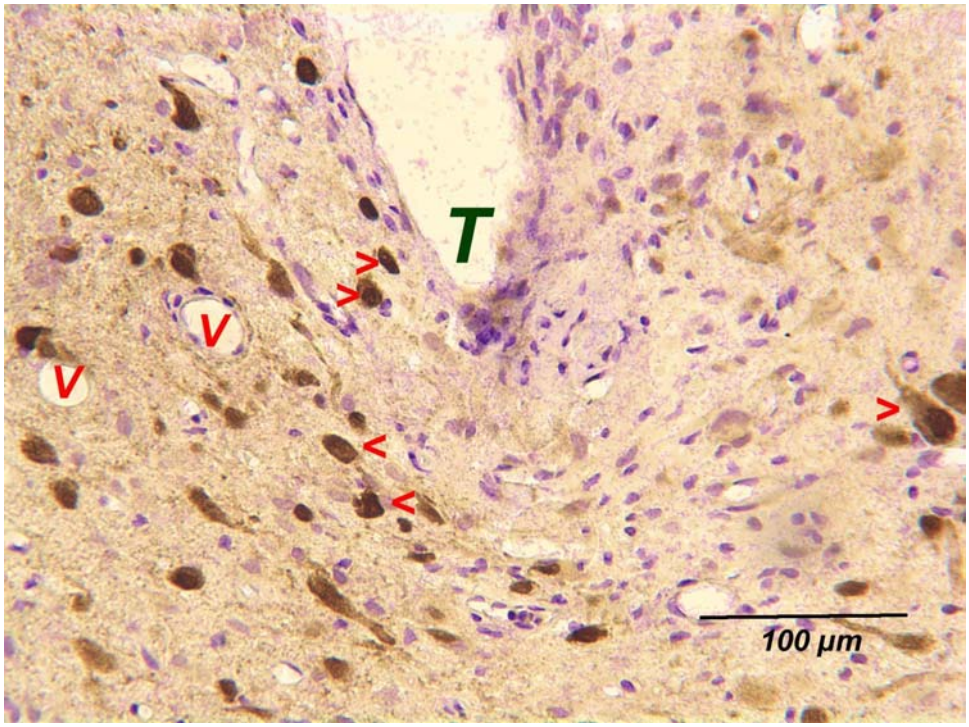

Figure 7. SP128, unpulsed electrode 5. This section show the tip (T) of the electrode capsule. Note the NeuN-positive neurons and neuronal processes (**< >**), capillaries (v) adjacent to the electrode capsule and an infiltration of glia cells ventral to the tip. NeuN-peroxidase immunoreaction with Nissl counter stain.

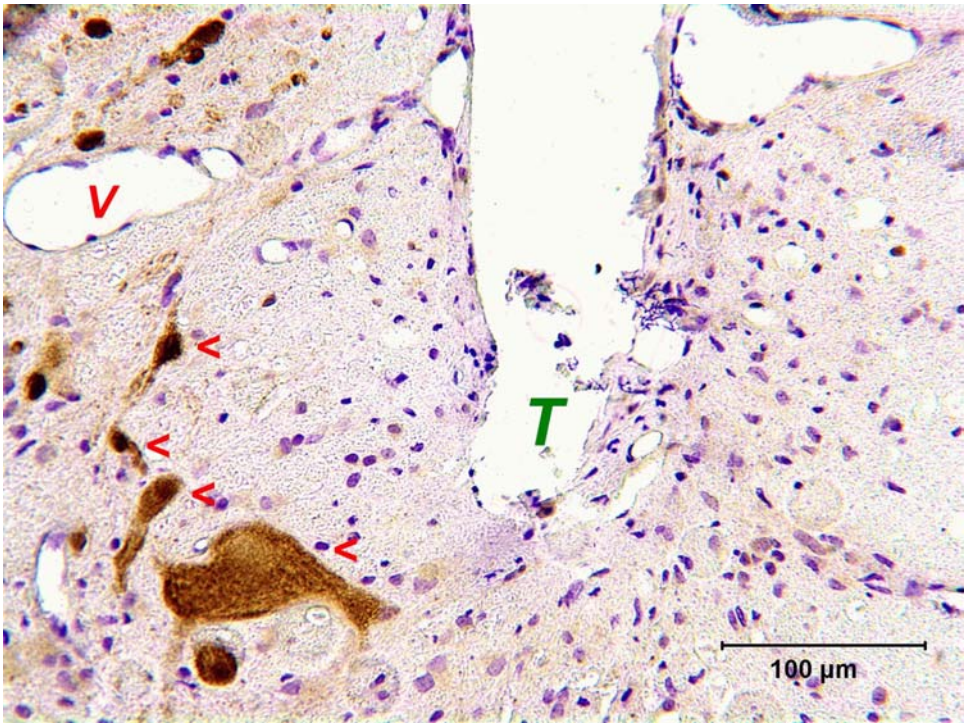

Figure 8. SP128, pulsed electrode 3. The tip (T) of the electrode is shown. Note the NeuN-positive neurons and neuronal processes (**<**), and a thin-walled blood vessel (v). A few blue-colored leukocytes can be seen adjacent to the electrode capsule. NeuN-peroxidase immunoreaction with Nissl counter stain.

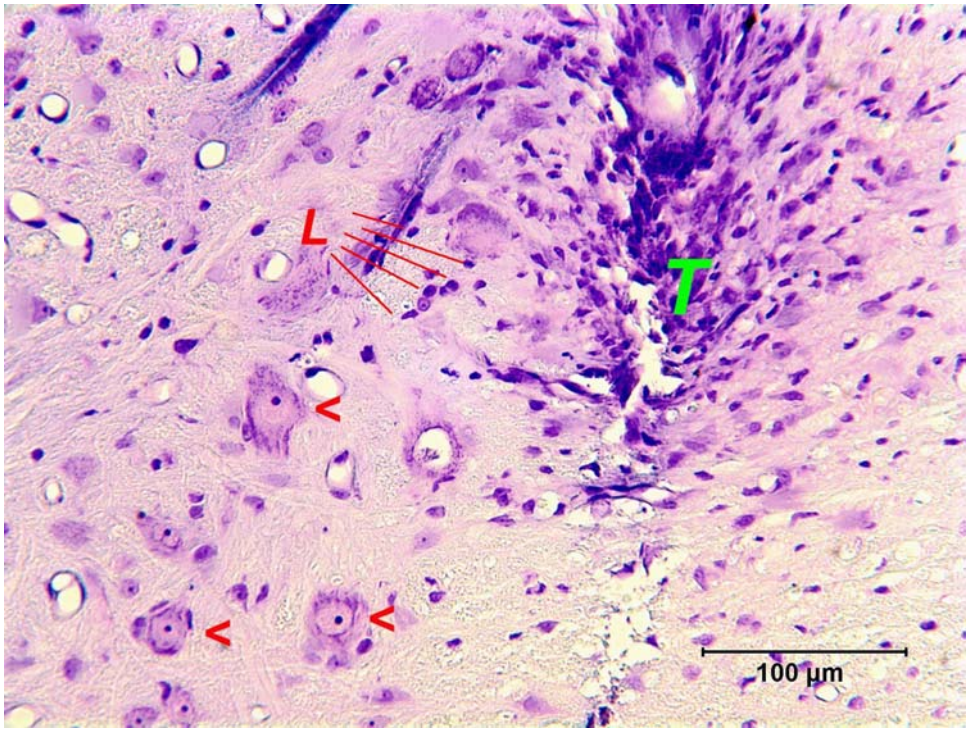

Figure 9. SP128, pulsed electrode 1. A grazing cut through the electrode capsule and adjacent to the site of the tip (T). Note the normal appearing neurons (<) and a few scattered, small, round leukocytes (L) amongst the glial cells surrounding the electrode capsule. Nissl stain.

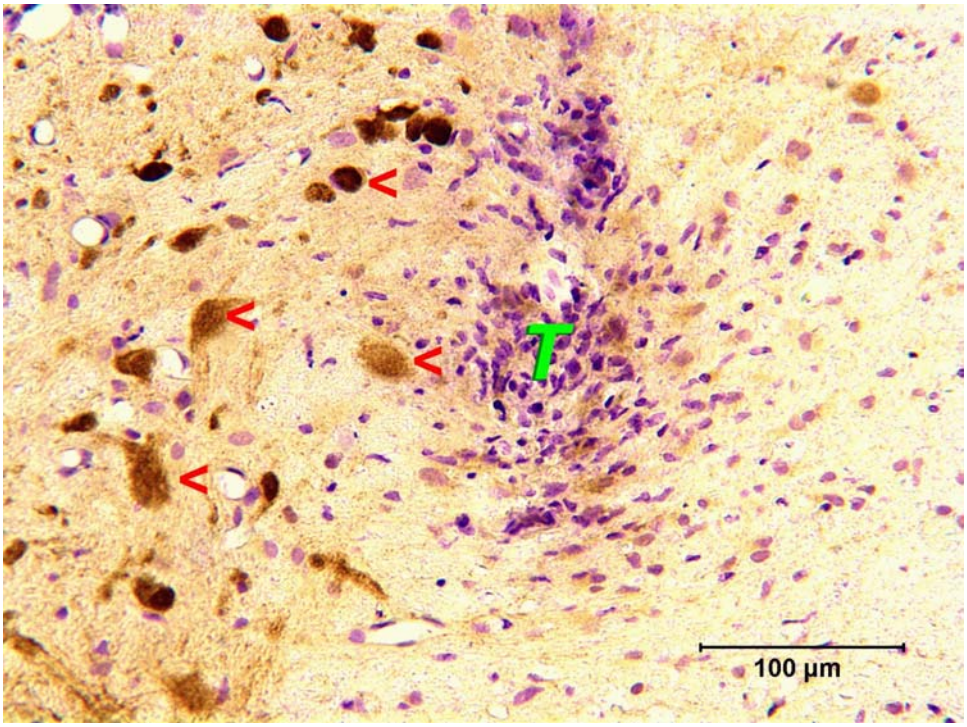

Figure 10. SP128, pulsed electrode 1. This is a section approximately 16 ：m lateral of the tip (T) of the same electrode shown in Figure9. Note the good differentiation between the brown-colored, NeuN-positive neuronal cell-bodies and processes (<), and the scattered blue-colored leukocytes amongst the glial cells surrounding the electrode tip. NeuN-peroxidase immunoreaction with Nissl counter stain.

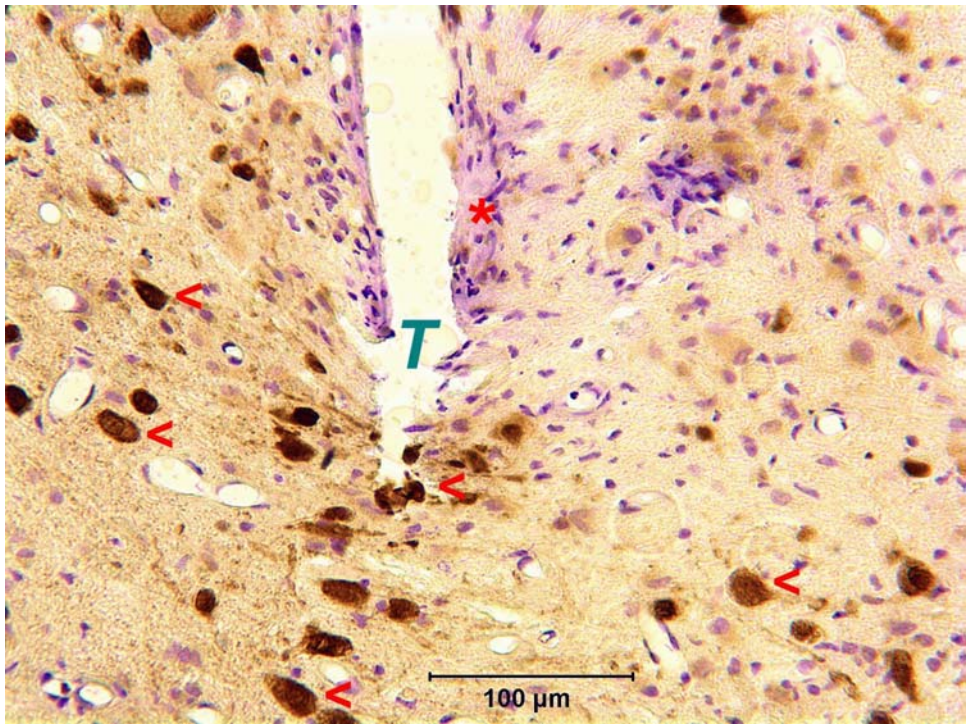

Figure 11. SP128. A section through the tip site (T) of unpulsed electrode 6. Note the differentiation between the brown-colored NeuN-positive neurons and neuronal processes (< >), and the blue-colored leukocytes and glial processes within the capsule and in association with the tissue adjacent to the capsule ( ). NeuN-peroxidase immunoreaction with Nissl counter stain.

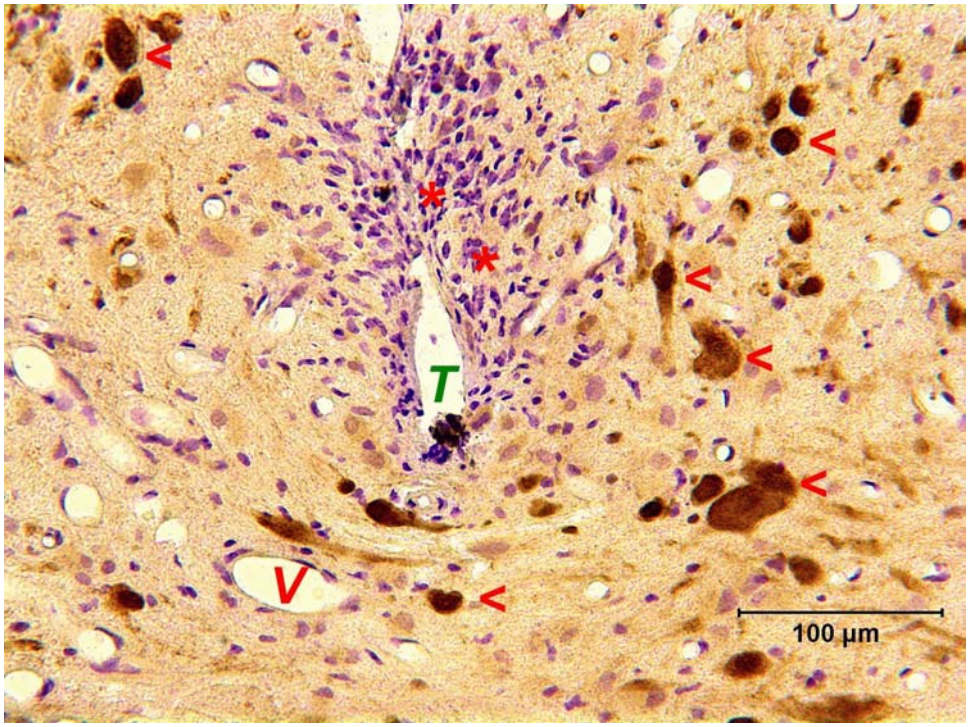

Figure 12. SP128, unpulsed electrode 7. This section shows the tip (T) and brown-colored NeuN-positive neurons and neuronal processes (<), and the blue-colored glial cells ( ) of a scar-like formation dorsal to the tip. Few if any lymphocytes are interspersed amongst the glial cells. NeuN-peroxidase immunoreaction with Nissl counter stain.

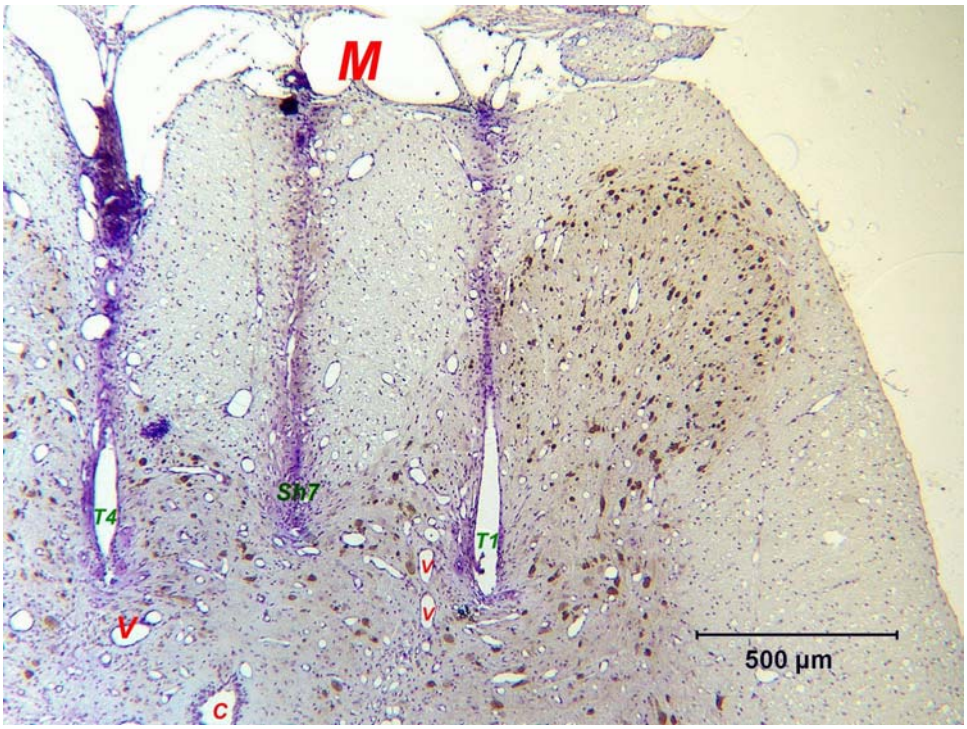

Figure 13. SP129. A view of a portion of the dorsolateral S_2 cord. Note the tracks and sheaths produced by electrodes 4, 1 and 7 (from left to right). The dorsal meningeal surface (M) has been flattened by the underside of the array superstructure. Small blood vessels (v) and the central canal (C) are also shown. NeuN-peroxidase immunoreaction with Nissl counter stain.

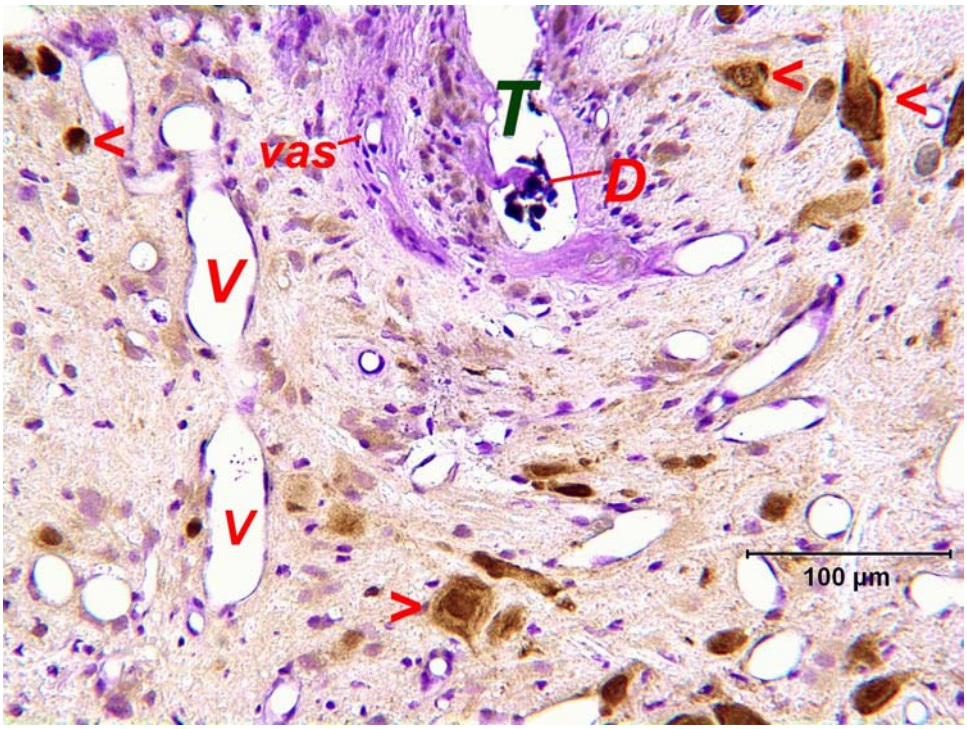

Figure 14. SP129, pulsed electrode 1. This section shows the tip site (T) and brown-colored NeuN-positive neurons and neuronal processes (**< >**). A deposit of optically dense material (D) at the tip of the track may be exfoliated iridium. The blue-colored glial cells and the capsule around the electrode shaft are interspersed with a few leukocytes. Blood vessels (V) are shown, one of which exhibits vasculitis (vas). NeuN immunoreaction with Nissl counter stain.

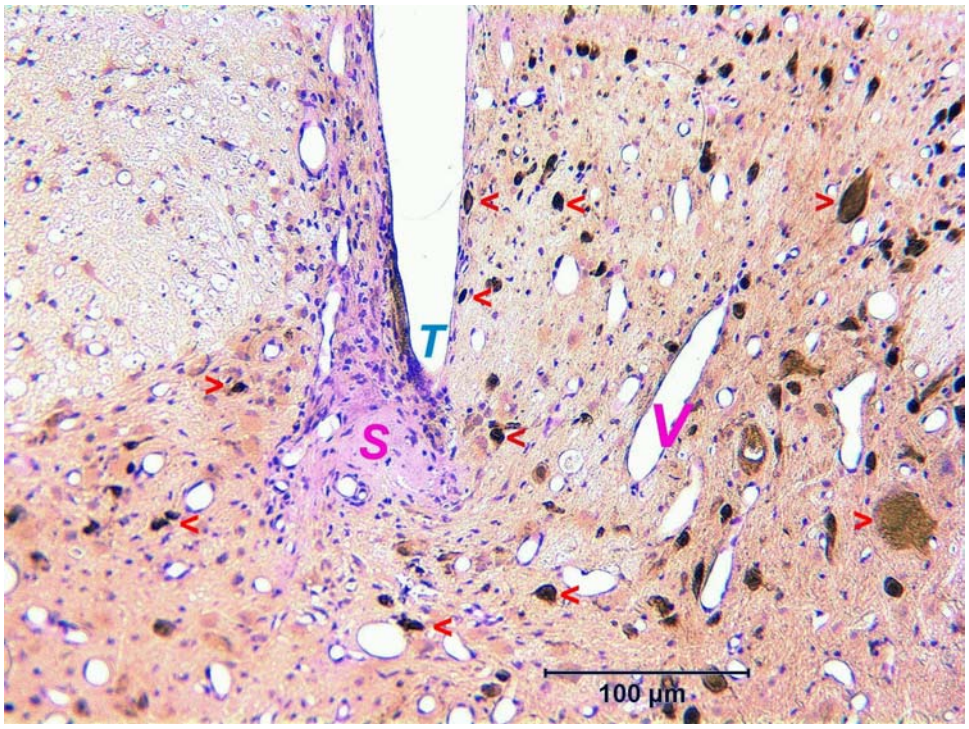

Figure 15. SP129, unpulsed electrode 2. This section shows the electrode tip (T), brown-colored NeuN-positive neurons and neuronal processes (**< >**), some very close to the electrode shaft. A glial scar (S), about 75 : m in width, is ventral to the tip site. The scar contains few, if any leukocytes and no neurons. Blood vessels (V) are also shown. NeuN-peroxidase immunoreaction with Nissl counter stain.

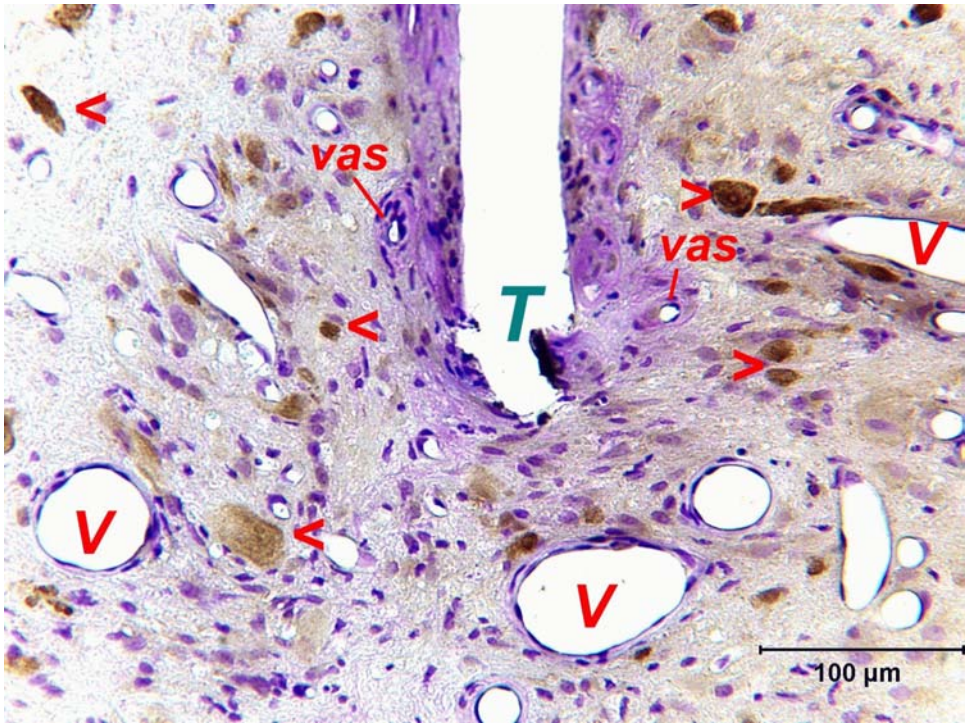

Figure 16. SP129, pulsed electrode 4. This section shows the electrode tip (T) surrounded by a thickened, more darkly stained capsule/glial scar that includes several vessels exhibiting vasculitis (vas). Brown-colored, NeuN-positive neurons and neuronal processes (< >) are also shown, as are blood vessels (V). NeuN-peroxidase immunoreaction with Nissl counter stain.

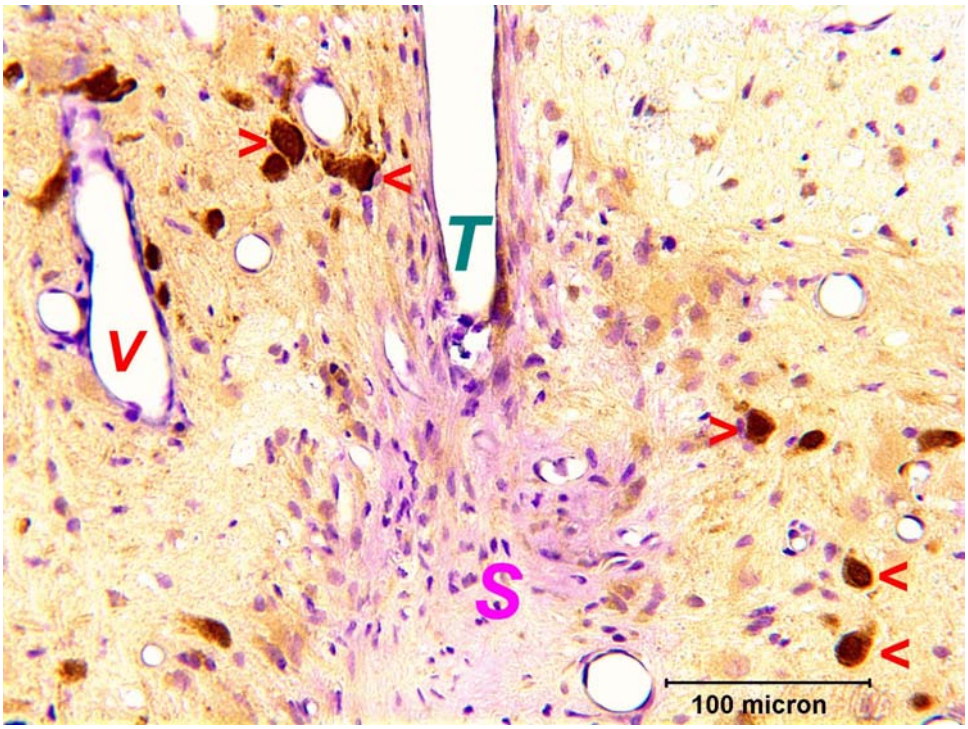

Figure 17. SP129, unpulsed electrode 5. This section shows the electrode tip (T), brown-colored NeuN-positive neurons and neuronal processes (< >) and a glial scar (S) about 150 μm in width, extending ventral to the tip site. The scar contains few, if any leukocytes and no neurons. Blood vessels (V) are also shown. NeuN-peroxidase immunoreaction with Nissl counter stain.

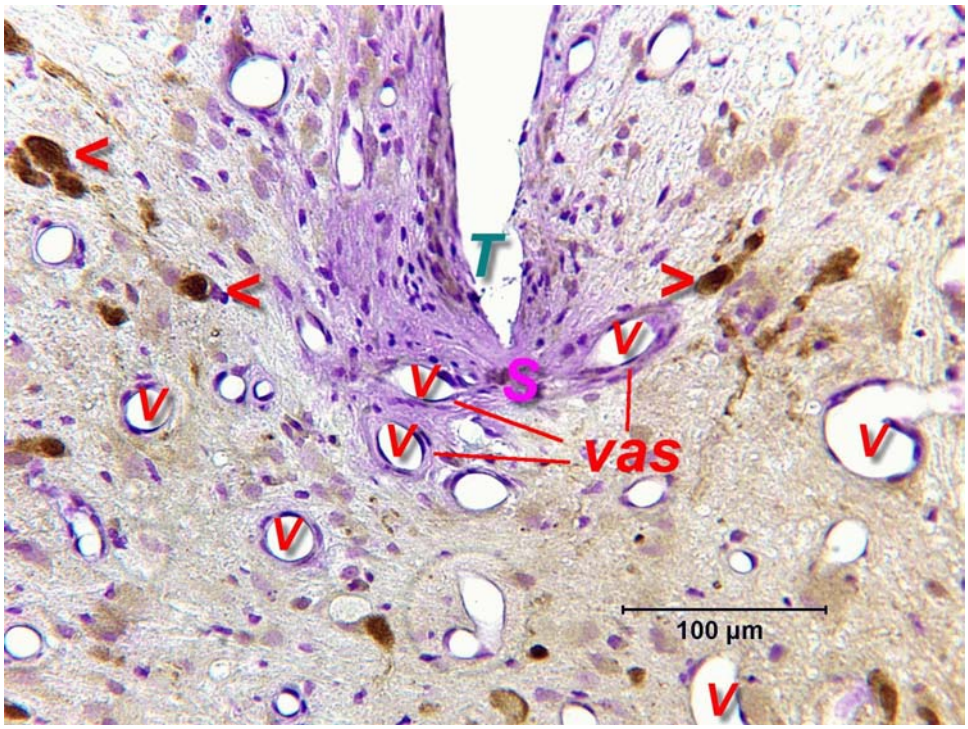

Figure 18. SP129, pulsed electrode 7. This section shows the electrode tip (T), brown-colored NeuN-positive neurons and neuronal processes (**< >**) and a glial scar (S) containing scattered blue-colored glial cells and a few leukocytes. The scar is darkly stained but unlike electrode 5 (Figure 17), does not extend far below the tips site. Blood vessels (V) are shown, and some close to the tip are expressing vasculitis (Vas). NeuN-peroxidase immunoreaction with Nissl counter stain.

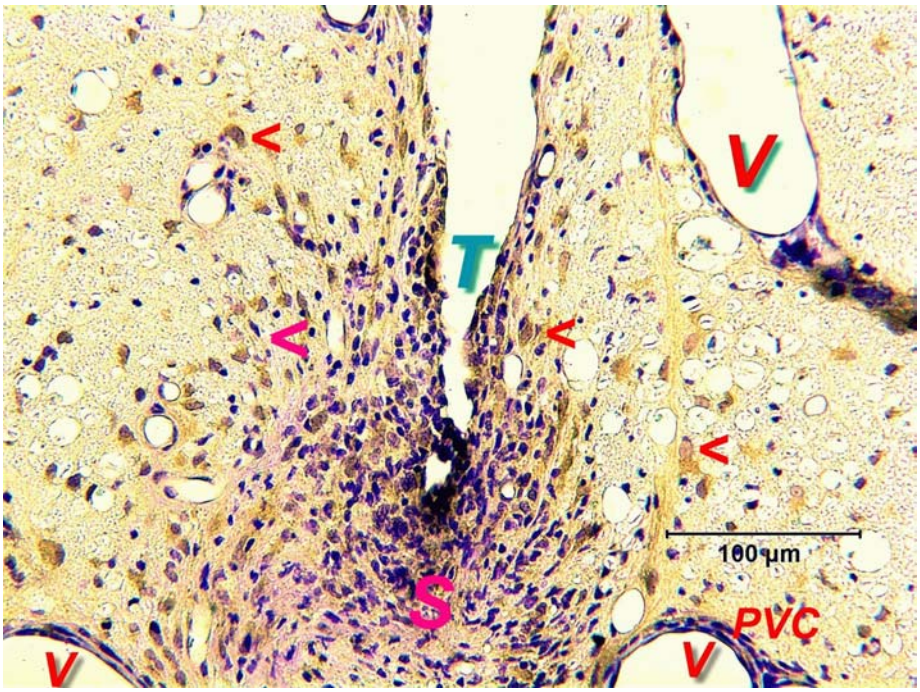

Figure 19. SP129, pulsed electrode 9. This section shows the electrode tip (T), yellow-brown-colored NeuN-positive neurons and neuronal processes (**< >**) and a glial scar (S) containing a mixture of glial cells and leukocytes. At least two of the blood vessels (V) exhibit perivascular cuffing of lymphocytes (PVC). This electrode tip was located in white matter (ventral part of the dorsal column dorsal to the central canal), and this may account for the more severe tissue damage at the tip site. NeuN-peroxidase immunoreaction with Nissl counter stain.